Lariat-Type B_{12} Model Complexes. 1. New Pendant Methylpyridyl Costa-Type Organocobalt Complexes Provide Insight into the Role of the Axial Ligand in Butterfly Bending and Redox Properties

Alessandra Gerli,[†] Michal Sabat,[‡] and Luigi G. Marzilli*,[†]

Contribution from the Department of Chemistry, Emory University, Atlanta, Georgia 30322, and Department of Chemistry, University of Virginia, Charlottesville, Virginia 22901.
Received November 25, 1991. Revised Manuscript Received May 1, 1992

Abstract: A new B_{12} (cobalamin, Cbl) model system with the potentially quinquedentate ligand, 2,3,9,10-tetramethyl-6,2-pyridylmethyl-1,4,8,11-tetraazaundeca-1,3,8,10-tetraen-1,11-diolo (C_1py), has unique properties attributable to the coordinated pendant pyridine, which is attached covalently at the 2-position by a one-methylene link to the central C of the propylene chain of (DO)(DOH)pn (N^2,$N^{2'}$-propanediylbis(2,3-butanedione 2-imine 3-oxime)). Treatment of C_1py, constructed from the new diamine, 2-(2-pyridylmethyl)-1,3-propanediamine, with hydrated $CoBr_2$ afforded $[BrCo(C_1py)]ClO_4$ (**5**). From **5**, salts of $[XCo(C_1py)]^+$ (X = CN, N_3, Cl) and of $[RCo(C_1py)]^+$ (R = CH_3, *i*-C_3H_7, *neo*-C_5H_{11}, CH_2CF_3) were synthesized by substitution and by oxidative addition of RX to in situ generated $Co^I(C_1py)$, respectively. In contrast to previous model systems, the C_1py model behaves more like Cbls; for example, no dicyano complex was obtained. Coordination of the pyridyl moiety in the C_1py derivatives is confirmed by X-ray structural analysis of $[ClCo(C_1py)]PF_6$ (**7**) and $[CH_3Co(C_1py)](ClO_4/BF_4)$ (**9a**). The pendant arm forces the pyridine to adopt an orientation 90° different from that in the [pyCo((DO)(DOH)pn)Cl(or R)]PF_6 derivatives. This new orientation greatly decreases butterfly bending, a structural feature relevant to triggering of Co–C bond homolysis by B_{12} enzymes. This result is strong evidence that a planar N-donor ligand can induce butterfly bending. In **7** the axial Co–N distance is 1.959 (4) Å, shorter than this distance (2.06 (1) and 2.07 (1) Å, for two independent molecules) in **9a** and similar to that in [pyCo((DO)(DOH)pn)Cl]PF_6. Although electrochemical reduction of the latter was not reversible, the reversible formation of Co(II) and Co(I) species from **7** (and **5**) can be attributed to the pendant nature of the axial pyridine. The Co(III)/Co(II) redox couple was more cathodic for **7**, consistent with better electron donation by the pendant pyridine. The Co(II)/Co(I) redox potential (−1.0 V vs 0.01 M Ag^+/Ag) of **7** and **5** was similar to that for nonalkyl (DO)(DOH)pn derivatives, which lack a pendant base; this suggests that Co(II)/Co(I) reduction in nonalkyl C_1py derivatives proceeds through a base-off form in which the Co–pyridine interaction is weak, at best. Such a mechanism was proposed previously for Cbls. For both $[CNCo(C_1py)]ClO_4$ and cyanoCbl (vitamin B_{12}), a single two-electron wave was observed upon reduction. For alkylC_1py derivatives, only one cathodic wave was observed upon reduction. Just one prominent cathodic peak has been reported for alkylCbls. For $[CH_3Co(C_1py)]ClO_4$ (**9**), reduction formed a dealkylated Co(I) species, which was oxidized to Co(II) on the reverse anodic scan. Similarly, dealkylated Co(I) species formed after one-electron reduction of alkylCbls, including methylCbl, are oxidized to Cbl(II) in the return anodic scan. The Co(III)/Co(II) reduction potentials of C_1py and Cbl derivatives were influenced nearly identically by changes in the axial ligand; for R(or X) = solvent, Cl, CN, *neo*-C_5H_{11}, CH_3, an excellent correlation with a slope of unity was obtained. The simpler chemistry of the C_1py derivatives, as illustrated here by electrochemical studies, makes them excellent models to study fundamental chemistry relevant to Cbls.

Introduction

In the three decades since the discovery that coenzyme B_{12}, a biologically active form of vitamin B_{12}, is an organocobalt complex,[1] a significant effort has been devoted to the synthesis and characterization of simple cobalt complexes containing a stable Co–C σ bond.[2-14] Studies on such compounds have aided the elucidation of the chemistry and biochemistry of cobalamin (Cbl) B_{12} coenzymes, including the two coenzymes important in human metabolism, 5′-deoxyadenosylcobalamin (AdoCbl) and methylcobalamin (MeCbl).[15,16] In particular, factors that influence the Co–C bond stability in such models have provided valuable insights into the homolysis of the Co–C bond,[2-8,17,18] a key step in catalytic cycles involving the protein-bound 5′-deoxyadenosyl cofactor.[2,15,17-21] However, in many ways, the model compounds actually exhibit *more complex chemistry* than the much larger natural products.

Strong evidence exists that homolysis is triggered by a conformational change induced in the coenzyme by the enzyme.[19] Butterfly bending is the most frequently advanced conformational change suggested, but there is little evidence in models that planar N ligands can induce significant butterfly bending.[2,3] The relationship between butterfly bending[2-4] and Co–C bond dissociation energy (BDE) estimated both kinetically and thermodynamically[7] represents one of the most important contributions of model chemistry toward understanding the conformational triggering of Co–C homolysis.[7] However, the most significant examples of such bending and the correlating Co–C BDE information involve phosphine ligands,[2-4,7] which have significantly different shapes

[†] Emory University.
[‡] University of Virginia.

(1) Lenhert, P. G.; Hodgkin, D. C. *Nature (London)* **1961**, *192*, 937.
(2) Randaccio, L.; Bresciani-Pahor, N.; Zangrando, E.; Marzilli, L. G. *Chem. Soc. Rev.* **1989**, *18*, 225.
(3) Bresciani-Pahor, N.; Forcolin, M.; Marzilli, L. G.; Randaccio, L.; Summers, M. F.; Toscano, P. J. *Coord. Chem. Rev.* **1985**, *63*, 1 and references cited therein.
(4) (a) Trogler, W. C.; Marzilli, L. G. *J. Am. Chem. Soc.* **1974**, *96*, 7589. (b) Trogler, W. C.; Marzilli, L. G. *Inorg. Chem.* **1975**, *14*, 2942. (c) Randaccio, L.; Bresciani-Pahor, N.; Toscano, P. J.; Marzilli, L. G. *J. Am. Chem. Soc.* **1980**, *102*, 7372. (d) Bresciani-Pahor, N.; Randaccio, L.; Toscano, P. J.; Marzilli, L. G. *J. Chem. Soc.* **1982**, 567. (e) Summers, M. F.; Toscano, P. J.; Bresciani-Pahor, N.; Nardin, G.; Randaccio, L.; Marzilli, L. G. *J. Am. Chem. Soc.* **1983**, *105*, 6259. (f) Nie, S.; Marzilli, P. A.; Marzilli, L. G.; Yu, N.-T. *J. Am. Chem. Soc.* **1990**, *112*, 6084.
(5) (a) Marzilli, L. G.; Summers, M. F.; Bresciani-Pahor, N.; Zangrando, E.; Charland, J.-P.; Randaccio, L. *J. Am. Chem. Soc.* **1985**, *107*, 6880. (b) Summers, M. F.; Marzilli, L. G.; Bresciani-Pahor, N.; Randaccio, L. *J. Am. Chem. Soc.* **1984**, *106*, 4478.
(6) (a) Parker, W. O., Jr.; Zangrando, E.; Bresciani-Pahor, N.; Randaccio, L.; Marzilli, L. G. *Inorg. Chem.* **1986**, *25*, 3489. (b) Parker, W. O., Jr.; Zangrando, E.; Bresciani-Pahor, N.; Marzilli, P. A.; Randaccio, L.; Marzilli, L. G. *Inorg. Chem.* **1988**, *27*, 2170. (c) Yohannes, P. G.; Bresciani-Pahor, N.; Randaccio, L.; Zangrando, E.; Marzilli, L. G. *Inorg. Chem.* **1988**, *27*, 4738. (d) Parker, W. O.; Bresciani-Pahor, N.; Zangrando, E.; Randaccio, L.; Marzilli, L. G. *Inorg. Chem.* **1985**, *24*, 3908.
(7) (a) Halpern, J. *Science* **1985**, *227*, 869. (b) Ng, F. T. T.; Rempel, G. L.; Mancuso, C.; Halpern, J. *Organometallics* **1990**, *9*, 2762. (c) Halpern, J.; Ng, F. T. T.; Rempel, G. L. *J. Am. Chem. Soc.* **1979**, *101*, 7124. (d) Ng, F. T. T.; Rempel, G. L.; Halpern, J. *J. Am. Chem. Soc.* **1982**, *104*, 621. (e) Tsou, T.-T.; Loots, M.; Halpern, J. *J. Am. Chem. Soc.* **1982**, *104*, 623. (f) Geno, M. K.; Halpern, J. *J. Am. Chem. Soc.* **1987**, *109*, 1238. (g) Geno, M. K.; Halpern, J. *J. Chem. Soc., Chem. Commun.* **1987**, 1052. (h) Ng, F. T. T.; Rempel, G.; Halpern, J. *Inorg. Chim. Acta* **1983**, *77*, L165.

0002-7863/92/1514-6711$03.00/0

Scheme I

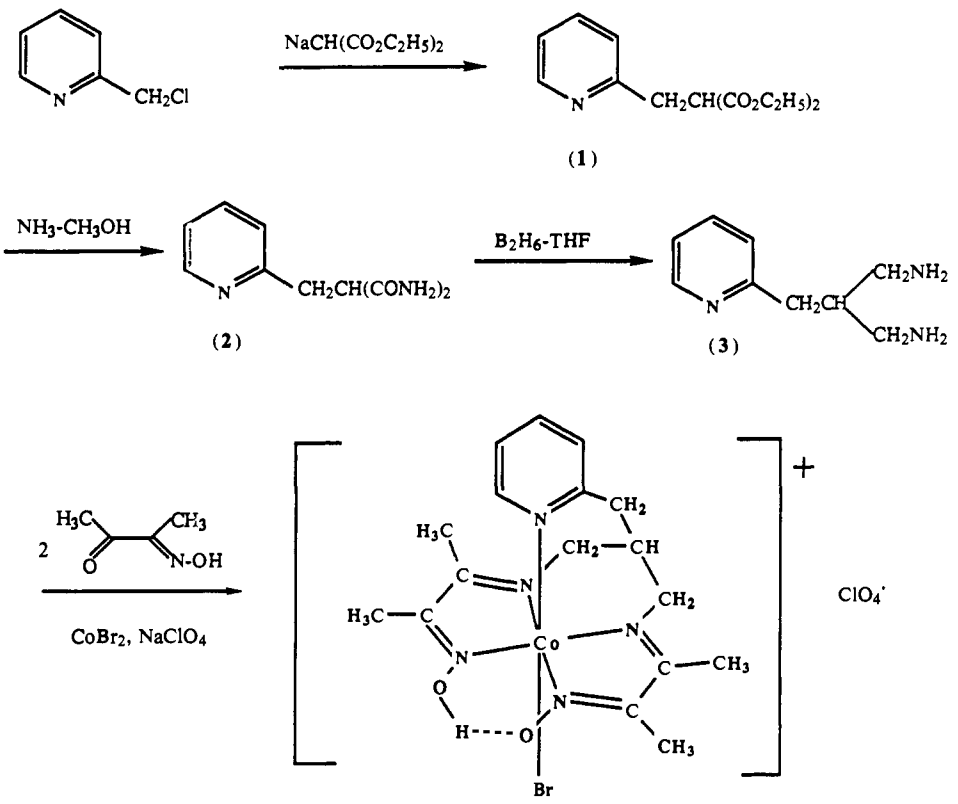

than the planar 5,6-dimethylbenzimidazole (DMBZ) ligand in Cbls.[21] Furthermore, the axial ligand in models is generally not linked to the equatorial ligand as in Cbls.[21]

The most extensively studied model systems (Figure 1) include cobaloximes,[3,4,7] $LCo(DH)_2R$ (DH = monoanion of dimethylglyoxime); Schiff base compounds like Co(saloph)R (saloph = dianion of disalicylidene-*o*-phenylenediamine);[5] and Costa-type derivatives[6,8,12-14,20] such as [LCo((DO)(DOH)pn)R]X and [LCo((EMO)(EMOH)pn)R]X [(DO)(DOH)pn $N^2,N^{2'}$-propanediylbis(2,3-butanedione 2-imine 3-oxime); (EMO)(EMOH)pn = a closely related system with the oxime methyl groups of (DO)(DOH)pn replaced by ethyl groups]. Of all these models, the Costa-type derivatives exhibit oxidation–reduction potentials[8,12-14,20] more similar to those of Cbls[16,22,23] and permit better modeling of some B_{12}-dependent enzymic rearrangements.[8,9,18]

Despite the important role these simple compounds have played in our understanding of these processes, the unidentate axial ligand is easily displaced. For example, CN^-, a strong ligand, tends to displace the axial ligand, and little data are available for comparisons with vitamin B_{12} itself. Also, the redox potential of Cbls is influenced by the appended axial base.[16] Electrochemical studies of models can be complicated by axial ligand loss, which creates a reactive site on the Co center.[8,13,14,20] For example, $[CH_3Co((DO)(DOH)pn)H_2O]ClO_4$[14,20] and $[CH_3Co((EMO)(EMOH)pn)H_2O]PF_6$[8] form $(CH_3)_2Co((DO)(DOH)pn)$ and $(CH_3)_2Co((EMO)(EMOH)pn)$, respectively, during electrochemistry. However, electrochemical studies on MeCbl do not mention such dialkyl products.[22,23]

We felt that complexes with a quinquedentate ligand would reflect the less complicated Cbl chemistry better. Synthetic ligands capable of imposing upon a metal a quinquedentate geometry consisting of a planar quadridentate group and a heterocyclic base are well-known,[24] but relevant Co complexes are rare.[25] We report

(8) (a) Finke, R. G.; Schiraldi, D. A.; Mayer, B. J. *Coord. Chem. Rev.* **1984**, *54*, 1. (b) Finke, R. G.; Smith, B. L.; McKenna, W. A.; Christian, P. A. *Inorg. Chem.* **1981**, *20*, 687. (c) Finke, R. G.; Schiraldi, D. A. *J. Am. Chem. Soc.* **1983**, *105*, 7605. (d) Finke, R. G.; McKenna, W. P.; Schiraldi, D. A.; Smith, B. L.; Pierpoint, C. *J. Am. Chem. Soc.* **1983**, *105*, 7592. (e) Elliott, C. M.; Hershenhart, E.; Finke, R. G.; Smith, B. L. *J. Am. Chem. Soc.* **1981**, *103*, 5558.

(9) (a) Muller, P.; Retey, J. *J. Chem. Soc., Chem. Commun.* **1983**, 1342. (b) Dowd, P.; Shapiro, M. *Tetrahedron* **1984**, *40*, 3063.

(10) Brown, D. G. *Prog. Inorg. Chem.* **1973**, *18*, 235.

(11) Alexander, V.; Ramanujam, V. V. *Inorg. Chim. Acta* **1989**, *156*, 125.

(12) Seeber, R.; Marassi, R.; Parker, W. O., Jr.; Marzilli, L. G. *Organometallics* **1988**, *6*, 1672.

(13) Gerli, A.; Marzilli, L. G. *Inorg. Chem.* **1992**, *31*, 1152.

(14) Seeber, R.; Marassi, R.; Parker, W. O., Jr.; Kelly, G. *Inorg. Chim. Acta* **1990**, *168*, 127.

(15) *B_{12}*; Dolphin, D., Ed.; Wiley & Sons: New York, 1982.

(16) Matthews, R. G.; Banerjee, R. V.; Ragsdale, S. W. *BioFactors* **1990**, *2*, 147.

(17) (a) Kim, S. H.; Chen, H. L.; Feilchenfeld, N.; Halpern, J. *J. Am. Chem. Soc.* **1988**, *110*, 3120. (b) Halpern, J.; Kim, S. H.; Leung, T. W. *J. Am. Chem. Soc.* **1984**, *106*, 8317. (c) Halpern, J. *Bull. Chem. Soc. Jpn.* **1988**, *61*, 13. (d) Halpern, J. *Pure Appl. Chem.* **1986**, *58*, 575.

(18) (a) Hay, B. P.; Finke, R. G. *J. Am. Chem. Soc.* **1986**, *108*, 4820. (b) Hay, B. P.; Finke, R. G. *J. Am. Chem. Soc.* **1987**, *109*, 8012. (c) Finke, R. G. In *Molecular Mechanisms in Bioorganic Processes*; Bleasdale, C., Golding, B. T., Eds.; The Royal Society of Chemistry: Cambridge, 1990; p 244. (d) Martin, B. D.; Finke, R. G. *J. Am. Chem. Soc.* **1990**, *112*, 2419.

(19) (a) Babior, B. M.; Krouwer, J. S. *Crit. Rev. Biochem.* **1979**, *6*, 35. (b) Wirt, M. D.; Sagi, I.; Chen, E.; Frisbie, S. M.; Lee, R.; Chance, M. R. *J. Am. Chem. Soc.* **1991**, *113*, 5299.

(20) Costa, G. *Pure Appl. Chem.* **1972**, *30*, 335.

(21) (a) Glusker, J. P. In *B_{12}*; Dolphin, D., Ed.; Wiley: New York, 1982; Vol. 1, Chapter 3, pp 23–106. (b) Pagano, T. G.; Marzilli, L. G.; Flocco, M. M.; Tsai, C.; Carrell, H. L.; Glusker, J. P. *J. Am. Chem. Soc.* **1991**, *113*, 531, and references cited therein.

(22) (a) Lexa, D.; Savéant, J.-M. *J. Am. Chem. Soc.* **1978**, *100*, 3220. (b) Faure, D.; Lexa, D.; Savéant, J.-M. *J. Electroanal. Chem.* **1982**, *140*, 297. (c) Lexa, D.; Savéant, J.-M.; Zickler, J. *J. Am. Chem. Soc.* **1980**, *102*, 2654. (d) Lexa, D.; Savéant, J.-M. *J. Am. Chem. Soc.* **1976**, *98*, 2652.

(23) Shepherd, R. E.; Zhang, S.; Dowd, P.; Choi, G.; Wilk, B.; Choi, S.-C. *Inorg. Chim. Acta* **1990**, *174*, 249.

(24) (a) Kimura, E.; Koike, T. *Comments Inorg. Chem.* **1991**, *11*, 285. (b) Kimura, E.; Koike, T.; Machida, R.; Nagai, R.; Kodama, M. *Inorg. Chem.* **1984**, *23*, 4181.

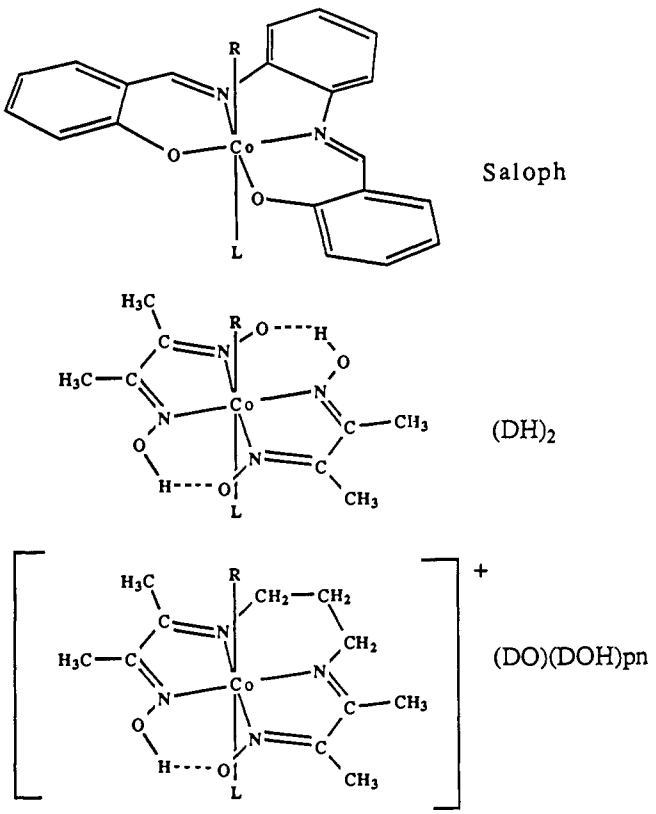

Figure 1. Structures of saloph, $(DH)_2$, and (DO)(DOH)pn derivatives.

here the synthesis and characterization of several alkyl and non-alkyl cobalt complexes of an unusual quinquedentate ligand composed of a pyridyl group attached through the 2-position by a one-methylene link to the central carbon of the propylene bridge of a (DO)(DOH)pn-type equatorial ligand.

Experimental Section

Reagents. $CoBr_2 \cdot xH_2O$ (40.5% H_2O) was purchased from Strem and $NaClO_4$ from Fisher. All other reagents were from Aldrich. Elemental analyses (Atlantic Microlabs, Atlanta, GA) and 300 MHz ^1H NMR spectral data are tabulated in the supplementary material.

Electrochemical Measurements. Cyclic voltammograms (CVs) were recorded as described previously.[13] Each voltammetric measurement was carried out using a 10^{-3} M solution of the complex in CH_3CN containing 0.1 M n-Bu_4NPF_6((TBA)PF_6). After each experiment, bis(cyclopentadienyl)iron(II) was added as an internal standard.[26] (Under our conditions, $E_{1/2}'$ for Fe(III)/(II) was +0.09 ± 0.01 V vs Ag/$AgNO_3$). For all complexes, CV scan rates ranged from 0.05–1 V/s, at 24 °C. Cathodic peak current (i_{pc}), anodic peak current (i_{ac}), separation between the anodic and cathodic peak potentials (ΔE_p), and half-wave potential ($E_{1/2}$) were computed.

Diethyl (2-Pyridylmethyl)malonate (1). The synthetic strategy is given in Scheme I. Over a 10-min period, diethyl malonate (43.25 mL, 256 mmol) was added to a solution of sodium ethoxide (5.405 g sodium 152 mmol, in 110 mL of absolute ethanol) in a 250-mL, three-necked flask equipped with a reflux condenser, dropping funnel, and nitrogen inlet. To the clear solution was then added gradually 2-picolyl chloride hydrochloride (15 g, 91 mmol). After the mixture had been heated under reflux for 4.5 h, the ethanol was removed by rotary evaporation. The residue was acidified with 4 N HCl (75 mL), with the temperature kept at ~0 °C during the addition. Treatment of the aqueous phase with 6 N NaOH (45 mL) at 0 °C precipitated an oil, which was then extracted with ether. The ether extracts were dried over sodium sulfate, filtered, and concentrated to a yellow oil (19 g, 87% yield).

(2-Pyridylmethyl)malondiamide (2). **1** (16 g, 64 mmol) was dissolved in methanol (80 mL), and a solution of ammonia in methanol (160 mL saturated at 0 °C) containing sodium methoxide (0.37 g, 6.9 mmol) was added. The product that separated as a white powder after 4 days was collected by vacuum filtration and vacuum-dried. A small second fraction, obtained by total removal of the solvent, was rinsed with ~50 mL of cold methanol and vacuum-dried: total yield, 11.95 g (97%).

2-(2-Pyridylmethyl)-1,3-propanediamine (3). To a suspension of **2** (10 g, 52 mmol) in 50 mL of tetrahydrofuran placed in a 500-mL, three-necked flask fitted with a magnetic stirrer, nitrogen inlet tube, dropping funnel, and condenser was added cautiously over 0.5 h a 1 M solution of B_2H_6·THF (240 mL). The flask was kept in an ice bath during the addition. Once the addition was complete, the ice bath was removed, and the mixture was brought to reflux and maintained there for 3 h. The reaction mixture was permitted to cool to room temperature, and the excess of diborane was destroyed by very cautious dropwise addition of distilled water (40 mL). The solution was evaporated to dryness on a rotary evaporator to yield a dry, white solid mass, which was slowly treated with 6 N HCl (200 mL). The resulting mixture was heated at reflux for 1 h and then taken to dryness on a rotary evaporator. The residue was dissolved in water (100 mL), and 6 N NaOH (70 mL) was added. The solution was extracted with $CHCl_3$ (4 × 200 mL). The combined $CHCl_3$ extracts were dried over magnesium sulfate, and the solvent was then evaporated to a clear oil (7.91 g, 93% yield). This amine is highly hygroscopic; it was converted to a hydrochloride salt (4) for analytical purposes.

2-(2-Pyridylmethyl)-1,3-propanediamine Trihydrochloride (4). Diamine **3** (1 g, 60 mmol) was added dropwise to a 1 M solution of HCl in diethyl ether (50 mL). A massive yellow precipitate immediately formed. Stirring was continued for 3 days until the yellow mass converted into a white solid, which was collected on a filter, rinsed with ethanol and then diethyl ether, and dried over phosphorus pentoxide (yield 0.98 g, 59%).

[BrCo(C_1py)]ClO_4 (5). To a solution of 2,3-butanedione monoxime (0.042 mol) in absolute ethanol (15 mL) placed in a 100-mL Schlenk flask was added slowly under N_2 and with constant stirring a solution of diamine **3** (3.47 g, 21 mmol) in absolute ethanol (30 mL). After 6 days of stirring under N_2, acetone (50 mL) and a solution of $CoBr_2 \cdot xH_2O$ (7.79 g) in water (20 mL) were added. The resulting brown mixture was stirred vigorously at room temperature and aerated with a current of air. After 3.5 h a solution of $NaClO_4$ (3.5 g, 25 mmol) in water (20 mL) was added. A brown solid precipitated after 2.5 h and was collected by vacuum filtration and washed with H_2O until the washings were nearly colorless (~50 mL); the product was then washed with diethyl ether (~50 mL) and dried in air (1.74 g, 14%).

[NCCo(C_1py)]ClO_4 (6). A red solution of **5** (0.5 g, 0.88 mmol, in 100 mL of aqueous methanol 1:1 v/v) and KCN (0.051 g, 0.79 mmol) in water (2 mL) was stirred for 10 min and then filtered. The volume was reduced to ~50 mL with a rotary evaporator (30 °C), and the solution was then extracted with 4 × 100 mL portions of CH_2Cl_2. Using a rotary evaporator, the CH_2Cl_2 layer was reduced to a brownish-yellow oily residue. Recrystallization from $CHCl_3$/hexanes afforded yellow needles (0.25 g, 38%).

[ClCo(C_1py)]PF_6 (7). A red solution of **5** (0.1 g, 0.18 mmol in 12 mL of aqueous methanol 1:5 v/v) in a 20-mL vial was treated with $AgNO_3$ (0.04 g, 0.24 mmol). The solution was stirred for 1 day, filtered to remove AgBr, and the filtrate was successively treated with LiCl (0.0035 g, 0.083 mmol) to remove the excess of $AgNO_3$. The next day the solution was refiltered and then treated with LiCl (0.0075 g, 0.18 mmol) and KPF_6 (0.04 g, 0.22 mmol). The vial was stoppered, and after 24 h red X-ray quality crystals formed (0.08 g, 80%).

[N_3Co(C_1py)]ClO_4 (8). A solution of **5** (0.25 g, (0.44 mmol) in 75 mL of aqueous methanol (1:2 v/v) was treated with NaN_3 (0.029 g, 0.44 mmol) in water (1 mL) and left uncovered in the hood. After 10 days well-formed red crystals were collected (0.13 g, 65%).

[RCo(C_1py)]ClO_4 (R = CH_3 (9), CF_3CH_2 (10), i-C_3H_7 (11), *neo*-C_5H_{11} (12)). Similar preparations were employed. For R = CH_3, a solution of NaOH (0.13 g) in H_2O (12.5 mL) was added to a brown suspension of **5** (0.5 g, 0.88 mmol) in methanol (75 mL) in a 125-mL Erlenmeyer flask, and the mixture was stirred vigorously until a red solution formed. Prepurified nitrogen was bubbled through the solution. A fresh solution of $NaBH_4$ (0.0338 g, 0.88 mmol) in water (10 mL) was added, followed by alkylating agent (0.11 mL, 1.76 mmol of iodomethane). The solution was stirred for 10 min, with N_2 passing over the solution. Acetone (10 mL) was then added to quench the BH_4^-, and the N_2 purging was stopped. After the solution was neutralized (pH 7) with 6 M HNO_3, the volume was reduced with a rotary evaporator (30 °C) until precipitation began. The orange powder collected by vacuum filtration was rinsed with diethyl ether, air-dried, and recrystallized twice from CH_2Cl_2/hexanes and vacuum-dried; yields were 40%–50%.

[CH_3Co(C_1py)]X (9a) (where X = $^5/_8ClO_4/^3/_8BF_4$). To the orange powder **9** (0.01 g, 0.02 mmol) was added water (3 mL), methanol (until

(25) (a) Collman, J. P.; Takaya, H.; Winkler, B.; Libit, L.; Koon, S. S.; Rodley, G. A.; Robinson, W. T. *J. Am. Chem. Soc.* **1973**, *95*, 1656. (b) Bernhardt, P. V.; Lawrance, G. A. *Coord. Chem. Rev.* **1990**, *104*, 297. (c) Tweedy, H. E.; Alcock, N. W.; Matsumoto, N.; Padolik, P. A.; Stephenson, N. A.; Busch, D. H. *Inorg. Chem.* **1990**, *29*, 616.

(26) Gritzner, G.; Kuta, J. *Pure Appl. Chem.* **1984**, *56*, 461.

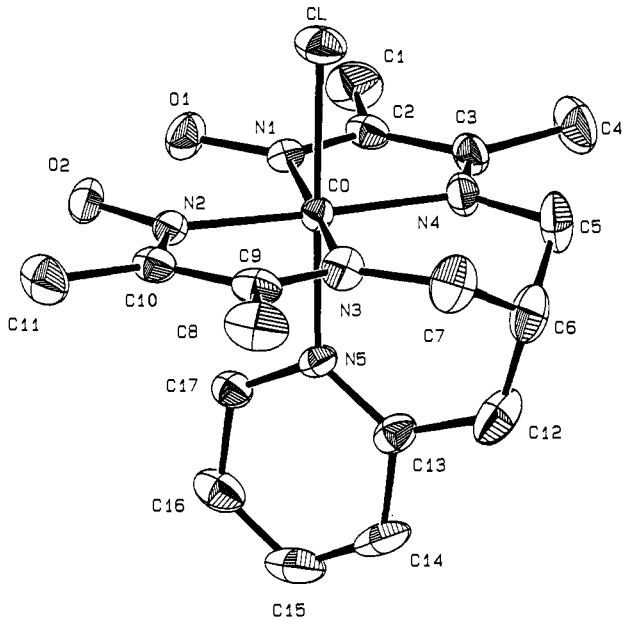

Figure 2. ORTEP drawing (50% probability thermal ellipsoids) and labeling scheme for the non-hydrogen atoms of $[ClCo(C_1py)]PF_6$ (7).

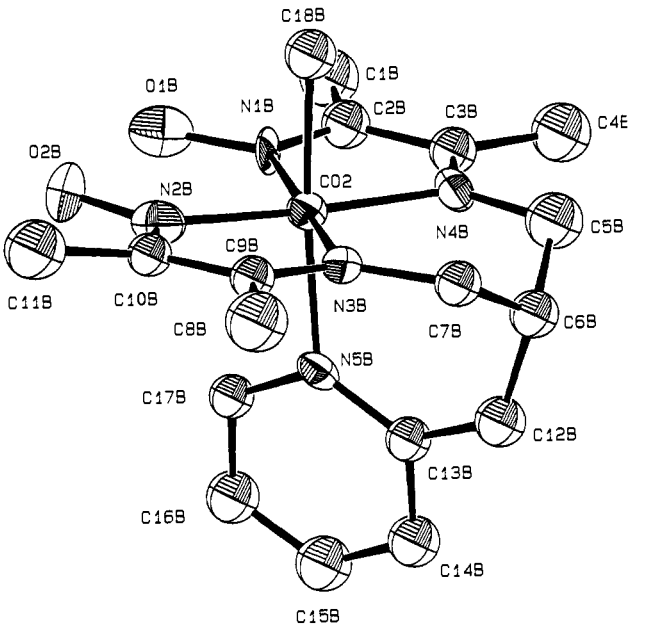

Figure 3. ORTEP drawing (50% probability thermal ellipsoids) and labeling scheme for the non-hydrogen atoms of $[CH_3Co(C_1py)]^5/_8ClO_4/^3/_8BF_4)$ (9a).

complete dissolution of the solid), and $NaBF_4$ (0.02 g, 0.2 mmol). The solution was filtered, and after 7 days at 5 °C, X-ray quality crystals were obtained. Several repetitions gave crystals containing the same percentage of ClO_4^-.

X-ray Data Collection and Structure Determination. All measurements were carried out on a Rigaku AFC6S diffractometer at 25 °C (calculations were performed on a Vaxstation 3520 computer using the TEXSAN 5.0 package).[27] Lattice parameters (Table I) for a 0.32 × 0.25 × 0.12 mm crystal of **7** and a 0.45 × 0.45 × 0.14 mm plate-like crystal of **9a** were determined by the least-squares refinement of the setting angles of 25 high-angle reflections. Intensities of three standard reflections measured every 100 reflections showed no changes.

Compound 7. An empirical absorption correction was applied by using ψ scans of several reflections with the χ angle close to 90°. Transmission factors were in the range 0.87–1.00. The structure was solved by heavy-atom techniques (Patterson and Fourier maps). The PF_6^- anion was found to be disordered between two sites, approximately related by a rotation of ~45° around an axis passing through P, having occupancies 0.75 and 0.25, respectively. Full-matrix least-squares refinement with anisotropic thermal parameters for all non-hydrogen atoms, including the disordered F atoms, yielded the final R of 0.040 (R_w = 0.046). The hydrogen atoms were located in the difference Fourier maps. The H atom involved in the intramolecular hydrogen bonding O(1)–H···O(2) was refined with an isotropic thermal parameter. The remaining H atoms were included as fixed contributions in the final cycles of refinement. The largest peak in the final difference map was 0.36 eÅ^{-3}. Final positional parameters are listed in the supplementary material.

Compound 9a. Systematic absences and preliminary calculations indicated the presence of eight molecules in the monoclinic space group $P2_1/c$ (no. 14). However, an elemental analysis showed the Co:Cl ratio was 1:0.65, indicating partial occupancy of the anions. An empirical ψ scan absorption correction was applied, with the transmission factors ranging from 0.83 to 1.00.

The structure was solved by direct methods (SIR88).[28] Since only two independent tetrahedral sites were found in the unit cell, it was assumed that they were occupied by the similar-size ClO_4^- ions and BF_4^- ions used in the metathesis reaction. This assumption was supported by the temperature factors found in preliminary refinements, which were abnormally high when Cl was the only central atom or negative when B was the only central atom. Population parameters for the Cl atoms were refined, giving values of 0.73 (2) and 0.53 (2) for ions A and B, respectively.

Full-matrix least-squares refinement with anisotropic thermal parameters for the Co, O, and N atoms of the cation gave the final R of 0.082

(27) TEXAN: Single Crystal Structure Analysis Software, Version 5.0 (1989); Molecular Structure Corporation, The Woodlands, TX 77381.

(28) SIR88: Burla, M. C.; Camalli, M.; Cascarano, G.; Giacovazzo, C.; Polidori, G.; Spagna, R.; Viterbo, D. *J. Appl. Cryst.* **1989**, *22*, 389.

Table I. Crystallographic Data for $[ClCo(C_1py)]PF_6$ (7) and $[CH_3Co(C_1py)]X$ (9a)

	7	9a
chemical formula	$CoClPF_6O_2N_5C_{17}H_{24}$	$CoO_{4.52}Cl_{0.63}N_5C_{18}H_{27}B_{0.37}F_{1.48}$
formula weight	569.76	499.15
space group	$P2_1/c$	$P2_1/c$
a, Å	8.322 (1)	15.042 (3)
b, Å	16.298 (2)	10.290 (4)
c, Å	16.846 (2)	28.749 (8)
β, deg	103.43 (1)	98.11 (2)
V, Å^3	2222.4 (9)	4406 (2)
Z	4	8
T, °C	25	25
λ (Mo Kα), Å	0.71069	0.71069
abs coeff, mm^{-1}	1.035	0.901
ρ_{calc}, g cm^{-3}	1.703	1.505
final R (R_w)	0.040 (0.046)	0.082 (0.098)

Table II. Selected Bond distances (Å) and Angles (deg) in 7 and 9a

Compound 7

Co–Cl	2.237 (2)	Co–N(2)	1.903 (4)	Co–N(4)	1.921 (4)
Co–N(1)	1.901 (4)	Co–N(3)	1.912 (4)	Co–N(5)	1.959 (4)

Cl–Co–N(1)	89.0 (1)	N(1)–Co–N(5)	92.4 (2)
Cl–Co–N(2)	89.1 (1)	N(2)–Co–N(3)	81.1 (2)
Cl–Co–N(3)	89.7 (1)	N(2)–Co–N(4)	177.4 (2)
Cl–Co–N(4)	89.7 (1)	N(2)–Co–N(5)	91.5 (2)
Cl–Co–N(5)	178.3 (1)	N(3)–Co–N(4)	101.2 (2)
N(1)–Co–N(2)	96.8 (2)	N(3)–Co–N(5)	88.9 (2)
N(1)–Co–N(3)	177.5 (2)	N(4)–Co–N(5)	89.8 (2)
N(1)–Co–N(4)	80.9 (2)		

Compound 9a

Co(1)–C(18A)	2.05 (2)	Co(1)–N(4A)	1.92 (1)	Co(2)–N(2B)	1.90 (1)
Co(1)–N(1A)	1.87 (1)	Co(1)–N(5A)	2.06 (1)	Co(2)–N(3B)	1.91 (1)
Co(1)–N(2A)	1.91 (1)	Co(2)–C(18B)	1.99 (2)	Co(2)–N(4B)	1.91 (1)
Co(1)–N(3A)	1.92 (1)	Co(2)–N(1B)	1.86 (1)	Co(2)–N(5B)	2.07 (1)

C(18A)–Co(1)–N(1A)	88.2 (6)	C(18B)–Co(2)–N(1B)	87.5 (6)
C(18A)–Co(1)–N(2A)	87.7 (6)	C(18B)–Co(2)–N(2B)	87.9 (7)
C(18A)–Co(1)–N(3A)	89.0 (6)	C(18B)–Co(2)–N(3B)	89.9 (6)
C(18A)–Co(1)–N(4A)	92.3 (6)	C(18B)–Co(2)–N(4B)	89.4 (6)
C(18A)–Co(1)–N(5A)	176.2 (6)	C(18B)–Co(2)–N(5B)	175.1 (6)
N(1A)–Co(1)–N(2A)	96.7 (6)	N(1B)–Co(2)–N(2B)	97.4 (6)
N(1A)–Co(1)–N(3A)	175.8 (6)	N(1B)–Co(2)–N(3B)	176.9 (6)
N(1A)–Co(1)–N(4A)	82.9 (6)	N(1B)–Co(2)–N(4B)	81.0 (6)
N(1A)–Co(1)–N(5A)	94.0 (5)	N(1B)–Co(2)–N(5B)	93.9 (5)
N(2A)–Co(1)–N(3A)	80.2 (6)	N(2B)–Co(2)–N(3B)	80.9 (6)
N(2A)–Co(1)–N(4A)	179.6 (6)	N(2B)–Co(2)–N(4B)	176.8 (6)
N(2A)–Co(1)–N(5A)	95.0 (5)	N(2B)–Co(2)–N(5B)	96.6 (5)
N(3A)–Co(1)–N(4A)	100.3 (5)	N(3B)–Co(2)–N(4B)	100.6 (6)
N(3A)–Co(1)–N(5A)	89.0 (5)	N(3B)–Co(2)–N(5B)	88.8 (5)
N(4A)–Co(1)–N(5A)	85.0 (5)	N(4B)–Co(2)–N(5B)	86.2 (5)

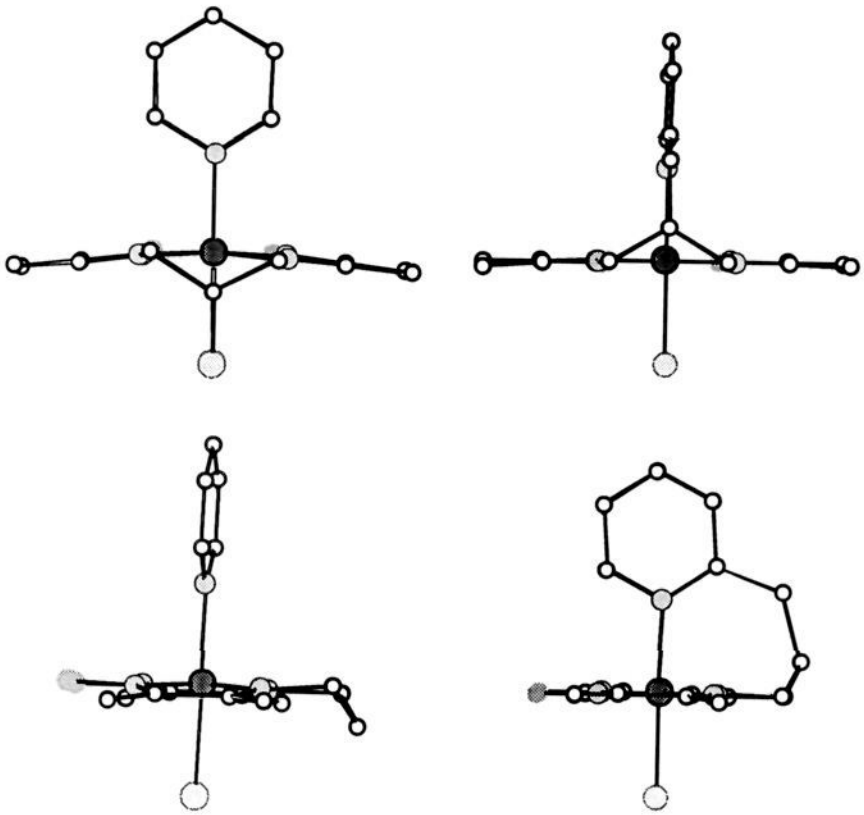

Figure 4. Ball and stick drawing of $[ClCo(C_1py)]PF_6$ (**7**) (right) and of $[pyCo((DO)(DOH)pn)Cl]PF_6$ (left) illustrating the differences in butterfly bending.

(R_w = 0.098). The H atom positions were calculated with a C–H distance of 1 Å and a H–C–H angle of 109.5°. The largest peak in the final difference map was 0.7 eÅ^{-3}. Final positional parameters are given in the supplementary material.

Results

Structural Studies. ORTEP drawings of cations **7** and **9a** (B) with the atom-numbering schemes are depicted in Figures 2 and 3. Selected bond lengths and angles are given in Table II. In both compounds cobalt exhibits a distorted octahedral stereochemistry. The C_1py ligand occupies the four equatorial positions and one axial position. Of particular note, the one-carbon bridge between the pyridine moiety and the central carbon of the propylene bridge supports pyridine coordination, but the two Co–N(axial)–C angles are not equivalent. For **7** the values for these two angles are 124.8(4)° for Co–N(5)–C(13) and 116.2(3)° for Co–N(5)–C(17). For **9a** the two angles are 128 (1)° for Co(1)–N(5A)–C(13A) and 116 (1)° for Co(1)–N(5A)–C(17A) and 126 (1)° for Co(2)–N(5B)–C(13B) and 112 (1)° for Co(2)–N(5B)–C(17B). For $[pyCo((DO)(DOH)pn)Cl]PF_6$, these angles are nearly equal and average ~122°.[13] The pyridine moiety is oriented with the α-H over the six-membered Co–N–O–H···O–N chelate ring. The N(5)–C(13)–C(12)–C(6) torsion angles are 4 (1)° for **7** and 3 (3)° (A) and −15 (3)° (B) for **9a**.

For **7** the four equatorial N atoms are coplanar within ±0.001 Å, and the cobalt is displaced 0.02 Å and C(6) 0.71 Å from this mean equatorial plane toward the axial nitrogen. For **7** the dihedral angle between plane N(1), C(2), C(3), N(4) and plane N(3), C(9), C(10), N(2) is 1.6°, with bending toward the axial chloride (Figure 4).

For **9a** the four equatorial N atoms are coplanar (±0.023 Å (A) and ±0.002 Å (B)) with C(6) displaced toward the axial nitrogen (0.68 Å (A), 0.71 Å (B)) from the plane. The cobalt is displaced in the same direction in B (0.04 Å) and is essentially coplanar in A (0.02 Å toward N).

For **9a** (A) the dihedral angle between plane N(1A), C(2A), C(3A), N(4A) and plane N(3A), C(9A), C(10A), N(2A) is 1.8°. Plane N(1A), C(2A), C(3A), N(4A) bends toward the axial nitrogen ligand. The dihedral angle between this plane and the equatorial plane is 2.6°. Plane N(3A), C(9A), C(10A), N(2A) bends toward the axial methyl ligand. The dihedral angle between this plane and the equatorial plane is 1.2°.

For **9a** (B) the dihedral angle between plane N(1B), C(2B), C(3B), N(4B) and plane N(3B), C(9B), C(10B), N(2B) is 4.4°. Plane N(1B), C(2B), C(3B), N(4B) bends slightly toward the axial methyl ligand. The dihedral angle between this plane and the equatorial plane is 0.3°. Plane N(3B), C(9B), C(10B), N(2B) bends toward the axial nitrogen ligand. The dihedral angle between this plane and the equatorial plane is 4.4°.

The size of the displacement of the central carbon of the propylene bridge from the equatorial plane is similar for C_1py and (DO)(DOH)pn derivatives (e.g., $[pyCo((DO)(DOH)pn)Cl]PF_6$, 0.62 Å[13]) but in the opposite direction. The similar C(5)–C(6) and C(6)–C(7) torsion angles in $[pyCo((DO)(DOH)pn)Cl]PF_6$ (−66.1° and +70.9°)[13] and in **7** (−72.5° and +72.9°) suggest that the propylene bridge in **7** is, at most, slightly more distorted.

Cyclic Voltammetry (cf. supplementary material and Table III). The CVs of $[BrCo(C_1py)]ClO_4$ (**5**) and $[ClCo(C_1py)]PF_6$ (**7**) (Figure 5) at 0.2 V/s are similar and exhibit two well-defined reduction waves, a quasi-reversible cathodic/anodic peak system at −0.6 V and a reversible cathodic/anodic peak system at −1.0 V. Although it shows chemical reversibility (i_{pa}/i_{pc} = 1), the Co(III)/Co(II) couple has a much slower rate of electron transfer (ΔE_p = 100 mV for **5** and 120 mV for **7** at 0.2 V/s) than the Co(II)/Co(I) couple (ΔE_p = 60 mV for **5** and **7** at 0.2 V/s). Slow electron transfer in the Co(III)/Co(II) couple for aquoCbl has been attributed to the increase in axial bond lengths accompanying reduction to Co(II).[10] In the CV of $[NCCo(C_1py)]ClO_4$ (**6**) at 0.2 V/s, a broad peak is observed at −1.04 V on the direct cathodic scan; a directly associated peak at −0.92 V can be detected on the reverse anodic scan.

In the CV of $[CH_3Co(C_1py)]ClO_4$ (**9**), the single cathodic peak at −1.54 V has no directly associated peak in the reverse anodic scan at all the scan rates attempted (0.05–1 V/s). Additional peaks at −0.97 and at +0.11 V (very small) in the reverse anodic scan do not shift with increased scan rate. The CV of

Table III. Cyclic Voltammetric Data[a] for C_1py Derivatives, Cobalamins, and Costa-type Derivatives

complex	redox couple	solvent	T (°C)	scan rate	E_{pc}	E_{pa}	$E_{1/2}$	ΔE_p	ref
$[BrCo(C_1py)]ClO_4$ (**5**)	III/II	CH_3CN	24	0.2	−0.57	−0.47	−0.52	100	
	II/I	CH_3CN	24	0.2	−1.03	−0.97	−1.00	60	
$[ClCo(C_1py)]PF_6$ (**7**)	III/II	CH_3CN	24	0.2	−0.63	−0.51	−0.57	120	
	II/I	CH_3CN	24	0.2	−1.03	−0.97	−1.00	60	
chlorocobalamin	III/II	DMSO	22	0.2			−0.48		22b
$[pyCo((DO)(DOH)pn)Cl]PF_6$	III/II	CH_3CN	24	0.2	−0.49				13
	II/I	CH_3CN	24	0.2	−1.04	−0.98	−1.01	60	
$[NCCo(C_1py)]ClO_4$ (**6**)		CH_3CN	24	0.2	−1.04	−0.92	−0.98	120	
cyanocobalamin	III/II	*b*	30.5	0.1	−1.29				22c
$[i\text{-}C_3H_7Co(C_1py)]ClO_4$ (**11**)		CH_3CN	24	0.2	−1.52	−1.34	−1.43	178	
$[i\text{-}C_3H_7Co((DO)(DOH)pn)H_2O]ClO_4$	III/II	CH_3CN	−17	0.2	−1.33		−1.25		14
	II/I	CH_3CN	−17	0.2	−1.51		−1.46		14
$[neo\text{-}C_5H_{11}Co(C_1py)]ClO_4$ (**12**)		CH_3CN	24	0.2	−1.47	−1.37	−1.42	100	
neopentylcobalamin	III/II	DMF/H_2O	24.6	0.05			−1.67		23
$[neo\text{-}C_5H_{11}Co((DO)(DOH)pn)H_2O]ClO_4$	III/II	CH_3CN	−17	0.2	−1.37		−1.30		14
	II/I	CH_3CN	−17	0.2	−1.45		−1.42		14
$[CH_3Co(C_1py)]ClO_4$ (**9**)		CH_3CN	24	0.2	−1.54	−0.97			
methylcobalamin	III/II	*b*	−30	0.1			−1.89	100	22a
$[CH_3Co((DO)(DOH)pn)H_2O]ClO_4$	III/II	CH_3CN	−17	0.2	−1.42				14
$[CF_3CH_2Co(C_1py)]ClO_4$ (**10**)		CH_3CN	24	0.2	−1.37	−0.97			
$[CF_3CH_2Co((DO)(DOH)pn)H_2O]ClO_4$		CH_3CN	−17	0.2	−1.33				14
$[CH_3CNCo(C_1py)]^{2+}$		CH_3CN	24	0.2		+0.11			
aquocobalamin	III/II	H_2O	22	0.1			−0.33	450	22d
$[Co((DO)(DOH)pn)(H_2O)_2](ClO_4)_2$	III/II	CH_3CN	25	0.2			−0.02		32

[a] Potentials in V vs 0.01 M Ag^+/Ag; potentials reported vs SCE were converted using E = +0.29 V for 0.01 M Ag^+/Ag in CH_3CN vs SCE (Larson, R. C.; Iwamoto, R. T.; Adams, R. N. *Anal. Chim. Acta* **1961**, *25*, 371). [b] DMSO–propanol 4:5.

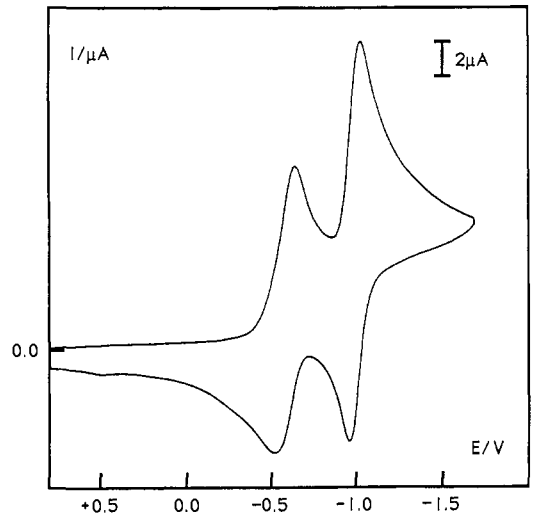

Figure 5. Cyclic voltammogram of $[ClCo(C_1py)]PF_6$ (**7**) at 0.2 V/s. Potential (E in V) is vs 0.01 M Ag^+/Ag.

$[CF_3CH_2Co(C_1py)]ClO_4$ (**10**) shows a profile similar to that of **9** at 0.2 V/s. However, at higher scan rates (0.5–1 V/s) the cathodic peak has a directly associated anodic peak at −1.37 V. For both **9** and **10**, an anodic peak was observed at −0.97 V, the E_{pa} for the Co(II)/Co(I) reduction of the nonalkyl derivatives **5** and **7**. Thus in both cases reduction is followed by dealkylation, leading to Co(I) species. The CV of $[i\text{-}C_3H_7Co(C_1py)]ClO_4$ (**11**) at 0.2 V/s shows a wave at −1.52 V in the reduction scan. The oxidation wave at −1.34 V can be partially resolved into two peaks at higher sweep rate (1 V/s). A single cathodic wave (−1.48 V) and a single anodic wave (−1.37 V) are observed in the CV of $[neo\text{-}C_5H_{11}Co(C_1py)]ClO_4$ (**12**).

Discussion

Structural Comparison. Some geometrical features of C_1py, (DO)(DOH)pn, and $(DH)_2$ analogues are compared in Table IV. The Co–N(pyridine) distance in $[CH_3Co(C_1py)]X$ (**9a**) is significantly longer than that in $[ClCo(C_1py)]PF_6$ (**7**), consistent with the electronic trans influence.[2-6,13] Although the Co–N axial bond length should also increase with the electron richness of the Co center,[2,3] the (DO)(DOH)pn compounds[6] were anomalous;

Table IV. Relevant Geometrical Data for C_1py Complexes and for the Analogous (DO)(DOH)pn and Cobaloxime Pyridine Complexes[a]

R(or X)	Co–R(or X), Å	Co–L, Å	α, deg	d, Å
		C_1py		
Cl[b]	2.237 (2)	1.959 (4)	+1.6	+0.02
CH_3[b] (A)	2.05 (2)	2.06 (1)	−1.8	+0.02
CH_3[b] (B)	1.99 (2)	2.07 (1)	−4.4	+0.04
		(DO)(DOH)pn		
Cl[c]	2.216 (6)	1.993 (6)	+13.0	+0.06
CH_3[d]	2.003 (3)	2.106 (3)	+6.9	+0.07
		Cobaloximes		
Cl[e]	2.229 (1)	1.959 (2)	+0.9	+0.03
CH_3[f]	1.998 (5)	2.068 (3)	+3.2	+0.04

[a] Positive values of α and d indicate that the bending of the equatorial ligand is toward X and that the displacement of Co out of the N4 equatorial donor set is toward L. [b] Present work. [c] Reference 13. [d] Reference 6d. [e] Randaccio, L., personal communication. [f] Bigotto, A.; Zangrando, E.; Randaccio, L. *J. Chem. Soc., Dalton Trans.* **1976**, 96.

the bond lengths were slightly longer than in cobaloximes, whereas our analysis of the solution properties suggested that the Co center is less electron rich than that in cobaloximes. Substitution of the oxime bridge in $(DH)_2$ derivatives with a propylene chain in (DO)(DOH)pn compounds increases the interaction with the axial ligand oriented as in A (Figure 6), so that it is forced into orientation B (Figure 6).[2,6,13] Steric clashes with the five-membered chelate ring in this orientation provoke a significant increase in Co–N bond length, compared with those in cobaloximes having the same axial ligands. When the axial pyridine in (DO)(DOH)pn derivatives is forced into orientation A through a link to the central carbon of the propylene bridge (C_1py derivatives), there is overall a slight decrease of Co–N bond lengths for the same R (or X). As a consequence, C_1py derivatives can adopt values of Co–N bond lengths comparable to those observed for cobaloximes.

Such differences in bond lengths are small compared to those in butterfly bending. For $[ClCo(C_1Py)]PF_6$ (**7**), the butterfly bending toward the axial Cl and displacement of cobalt toward the axial nitrogen ligand (Table IV and Figure 4) are small. For **9a**, the unsymmetrical butterfly bending is small in both independent molecules. Thus, both for C_1py and cobaloximes, where the orientation of the pyridine is A, butterfly bending is small. In (DO)(DOH)pn derivatives, butterfly bending is relatively large.[6,13] Substitution of Cl by CH_3 produces a relative decrease in butterfly bending (Table IV). Clearly, the shorter Co–N

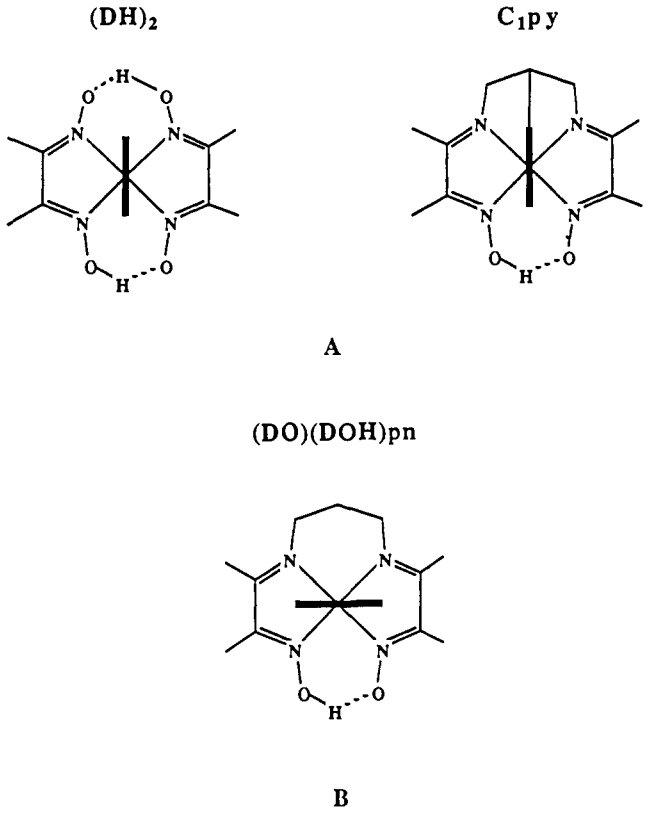

Figure 6. Eclipsed orientation of the pyridine plane in C_1py and $(DH)_2$ derivatives (A) and staggered orientation of the pyridine plane in (DO)(DOH)pn derivatives (B).

distance in the Cl derivative leads to greater steric interaction and hence butterfly bending.[13] Taken together, these results clearly demonstrate for the first time that butterfly bending can be caused by a planar N-donor ligand.

For a given R there is a striking absence of correlation of Co–C BDE[7,8,17,18] with any structural feature except Co–N (L) bond length.[2-6,21] This observation and the unusually long Co(III)–N (DMBZ) bond in B_{12} coenzymes[21,29] have led us to suggest that conformational changes involving *both* the corrin and the DMBZ may affect homolysis.[2,5] We speculated that a weak axial donor is needed to keep the Co(III) in the plane (and thus facilitate corrin-Ado nonbonded interactions). DMBZ donation is weakened by steric interactions. However, the DMBZ is needed to stabilize the Co(II) form after Co–C bond homolysis (and prevent Co–C bond formation to the substrate-derived radical).[5] The subsequent demonstration in an important structural study that the Co–N bond is long in Cbl^{II}[30] as is normal supports this speculation.

In a recent excellent study, Toraya and Ishida[31] synthetically replaced the α-D-ribofuranose ring in the Cbl nucleotide loop with a methylene chain, $-(CH_2)_n-$ where n = 2, 3, 4, and 6. When the axial ligand was CN, the base-on vs the base-off form was most favorable for the tetramethylene analogue. Thus, the length of the chain (four) in the natural Cbl appears optimal.

The activity found for diol dehydratase, as assessed either by k_{cat} or k_{cat}/K_m, was found to be greater for the Ado form of the n = 3 than the n = 4 analogue. There thus appeared to be no correlation between the strength of the Co–DMBZ interaction and activity. However, the base-on to base-off equilibrium was measured for the free derivatives. If, instead, an analysis of the equilibrium is made with λ_{max} values (~475 nm), then a case could be made that the trimethylene analogue exists in the base-on form in the "holoenzyme". The K_m value is greater by an order of magnitude for the tetramethylene analogue, although K_m for the trimethylene analogue is comparable to that for AdoCbl.[31]

These important results can be reinterpreted to suggest that a repositioning of the nucleotide loop is required for activity. The energy required diminishes K_m for AdoCbl. The repositioned DMBZ may correspond to the position of DMBZ in the trimethylene analogue, which consequently has a fairly large k_{cat}. It is not clear, however, whether such repositioning increases steric clashes with the corrin, enhancing or facilitating the corrin conformational distortion. We eagerly await structural studies on these new Cbl analogues.

Electrochemistry. The voltammetric profiles of $[BrCo(C_1py)]ClO_4$ (**5**) and $[ClCo(C_1py)]PF_6$ (**7**) (Figure 5) are similar. The Co(III)/Co(II) cathodic reduction of **7** (Table III) is 140 mV more cathodic than the E_{pc} = −0.49 V at 0.2 V/s for $[pyCo((DO)(DOH)pn)Cl]PF_6$,[13] which has an irreversible Co(III)/Co(II) cathodic process due to the loss of the axial py ligand.[13] The orientation of the pendant pyridine in **7** accounts for the cathodic shift, and the pendant ligand is responsible for the reversible formation of Co(II).

Studies on Cbls and on B_{12} models have demonstrated that the Co(II)/Co(I) couple is relatively insensitive to the axial ligands and, therefore, reflects primarily the electronic influence of the equatorial quadridentate ligand.[10] The Co(II)/Co(I) potential of −1.00 V for the nonalkyl C_1py derivatives, **5** and **7**, is similar to that for nonalkyl (DO)(DOH)pn derivatives without an axially ligated base (i.e. $E_{1/2}$ for $Co((DO)(DOH)pn)Br_2$ = −1.01 V).[32] This similarity suggests that in $Co^{II}C_1$py derivatives the pyridine moiety has either weak or no interaction with cobalt and that the halide has dissociated. Two CE mechanisms[22b] could also explain the results.

A single two-electron wave was observed upon reduction of $CNCbl^{III}$[22c] (CV in 4:5 DMSO–propanol, 30.5 °C, 0.1 V/s) at −1.29 V, corresponding to the direct formation of Cbl^{I}; a peak due to the oxidation of Cbl^{I} to Cbl^{II} was observed in the reverse anodic scan. It was proposed[22c] that $CNCbl^{III}$ is reduced in an ECE reaction sequence involving the following steps: (i) reduction of $CNCbl^{III}$to $CNCbl^{II}$, followed by loss of the axial cyanide and formation of Cbl^{II}; and (ii) reduction of base-off Cbl^{II} (in equilibrium with the base-on form) to Cbl^{I} at a potential more anodic than that of $CNCbl^{III}$.

In the CVs for $[NCCo(C_1py)]ClO_4$ (**6**) at 0.05 and 0.1 V/s, the cathodic peak is very broad and appears to be a composite of two peaks. At 0.2 V/s the CV has a single broad cathodic wave. However, a single sharp peak is observed in the CV at the faster scan rates of 0.5 and 1 V/s. This dependence suggests that the irreversible Co(III)/Co(II) reduction process occurs at a potential close to that of the Co(II)/Co(I) couple at low scan rates and moves cathodically at higher scan rates, so that an apparent direct two-electron reduction is observed. Therefore, the reduction process is similar to that observed for CNCbl. This interpretation of the voltammetric behavior of $[NCCo(C_1py)]ClO_4$ (**6**) suggests that the presence of a stronger nucleophile (CN^-) moves the potential of the Co(III)/Co(II) couple cathodically compared to **5** and **7**, with halide nucleophiles.

The CVs of $[CH_3Co(C_1py)]ClO_4$ (**9**) and MeCbl[23] are both characterized by the presence of one cathodic peak due to the reduction of the starting complex and by two anodic peaks in the reverse scan due to the Co(I)/Co(II) and Co(II)/Co(III) oxidations of dealkylated species. As a consequence, the voltammetric profiles of the two complexes are very similar.

The single cathodic wave at −1.6 V for $[CH_3Co^{III}((EMO)(EMOH)pn)H_2O]PF_6$ (25 °C, CH_3CN, excess *N*-methylimidazole)[8e] occurs at approximately the same potential as that for **9** (−1.54 V). The better electron donor *N* ligands make both compounds ~0.15 V more difficult to reduce than $[CH_3Co^{III}((DO)(DOH)pn)H_2O]ClO_4$ (E_{pc} = −1.42 V, CH_3CN, −17 °C),[14] with an axial CH_3CN. A similar shift in reduction potential was

(29) Rossi, M.; Glusker, J. P.; Randaccio, L.; Summers, M. F.; Toscano, P. J.; Marzilli, L. G. *J. Am. Chem. Soc.* **1985**, *107*, 1729.
(30) Krautler, B.; Keller, W.; Kratky, C. *J. Am. Chem. Soc.* **1989**, *111*, 8936.
(31) Toraya, T.; Ishida, A. *J. Biol. Chem.* **1991**, *266*, 5430.
(32) Seeber, R.; Parker, W. O., Jr.; Marzilli, P. A.; Marzilli, L. G. *Organometallics* **1989**, *8*, 2377.

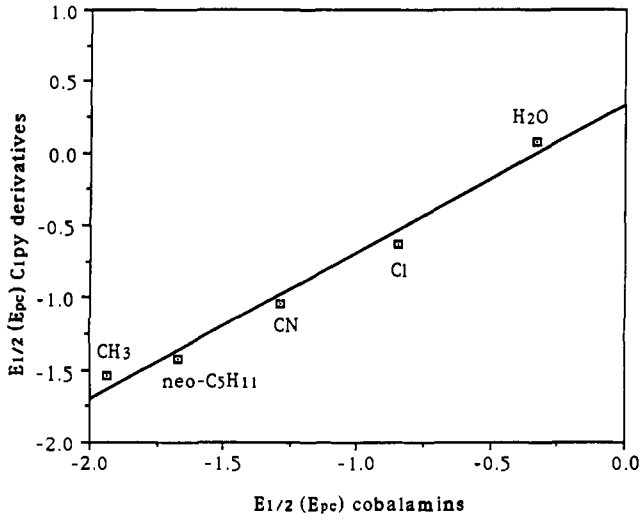

Figure 7. Plot of $E_{1/2}$ (E_{pc}) of C_1py derivatives vs $E_{1/2}$ (E_{pc}) of analogous cobalamins.[33]

observed between base-on MeCbl (−1.89 V)[22a] and base-off methylcobamide (−1.75 V).[22a]

It has been suggested that the reactivity of alkyl Co(II) derivatives is conditioned by the bulk of the alkyl group;[8,12,14] [*i*-C_3H_7Co((DO)(DOH)pn)H_2O]ClO_4[14] and [*neo*-C_5H_{11}Co((DO)(DOH)pn)H_2O]ClO_4[12,14] did not decompose via a bimolecular mechanism upon reduction. For these two compounds, the resolved two charge-transfer process suggests, first, the reduction of the starting alkyl Co(III) complex, and, second, the Co(II)/Co(I) reduction of a species in which presumably the alkyl group has migrated onto the equatorial ligand. Although both [*i*-C_3H_7Co(C_1py)]ClO_4 (**11**) and [*neo*-C_5H_{11}Co(C_1py)]ClO_4 (**12**) exhibit only one cathodic wave with a directly associated anodic wave and better reversibility than [CH_3Co(C_1py)]ClO_4 (**9**), the peaks shifted farther apart with increasing scan rate, and the ratio of the peak currents differed from unity (i_{pa}/i_{pc} = 0.66 for **11**; 0.71 for **12**), indicating that the electrochemical reductions were not fully reversible. Coordination of the axial base in **11** and **12** makes the first couple more cathodic than for the respective [RCo((DO)(DOH)pn)H_2O]ClO_4.[12] As for **11** and **12**, just one prominent cathodic peak was observed for alkylCbls.[22,23]

It is interesting to note that the Co(III)/Co(II) reduction potential of [CH_3Co(C_1py)]ClO_4 was more negative than those of [*i*-C_3H_7Co(C_1py)]ClO_4 and [*neo*-C_5H_{11}Co(C_1py)]ClO_4. The reduction potential of MeCbl (−1.89 V) was also more cathodic than that of neopentylCbl (−1.67 V).[23] It has been suggested that such a shift may reflect changes in the axial ligand distances which modulate the energy of the lowest σ-type MO (LUMO).[23] The shorter Co–C and Co–N(DMBZ) bonds in MeCbl should raise the energy of this MO relative to that in Cbls with bulky alkyl groups and longer axial bonds.[23] The higher energy of the LUMO in MeCbl would explain the trend in reduction potential.

A good correlation (slope = 1.01, correlation coefficient = 0.981) was obtained between the reduction potentials of analogous derivatives, C_1py vs Cbls for R(or X) = solvent, Cl, CN, *neo*-C_5H_{11}, CH_3 (Figure 7).[33] The slope near unity indicates that the Co(III)/Co(II) redox potentials are influenced in the same way by axial ligands. In this respect, C_1py derivatives are excellent models for Cbls.

Conclusions

The one-methylene link in [R(or X)Co(C_1py)]$^+$ complexes forces the pyridine to assume orientation A (Figure 6). Compared to analogous (DO)(DOH)pn derivatives, where py has orientation B, the resultant slight shortening of the Co–N(axial) distance in C_1py derivatives increases electron donation from the pyridine to the cobalt center and makes the Co(III)/Co(II) reduction more difficult.

The propylene bridge has a similar conformation in C_1py and (DO)(DOH)pn compounds, but the butterfly bending is greater in the latter. We attribute this difference to the different orientations (Figure 6). Our previous findings that the planar axial N ligands did not cause butterfly bending in cobaloximes can now be clearly attributed to orientation. Together, these results provide clear evidence that an N-donor ligand can induce butterfly bending.

The better electrochemical reversibility observed for C_1py than for (DO)(DOH)pn nonalkyl derivatives can be attributed to the pendant nature of the pyridine moiety in the C_1py complexes. For [ClCo(C_1py)]$^+$ and [BrCo(C_1py)]$^+$ the Co(II)/Co(I) $E_{1/2}$ is similar to that for nonalkyl (DO)(DOH)pn derivatives without an axially ligated base. This similarity suggests that the base-off form of [$Co^{II}C_1$py]$^+$ derivatives is reduced, as suggested also by studies on Cbls. For [CNCo(C_1py)]$^+$ and [RCo(C_1py)]$^+$ derivatives, the Co(III)/Co(II) and Co(II)/Co(I) reduction potentials are similar, and the cathodic waves often overlap. Typically, only one cathodic wave was observed also upon reduction of CNCbl or alkylCbls.

The presumably longer Co–C distance in [*neo*-C_5H_{11}Co(C_1py)]$^+$ leads to easier reduction than for [CH_3Co(C_1py)]$^+$ as also observed for methyl and neopentyl Cbls.[23] Co(III)/Co(II) reduction potentials of C_1py derivatives and Cbls are influenced similarly by axial ligands trans to the heterocyclic base, making these C_1py derivatives excellent electrochemical models of Cbls.

As judged by electrochemical methods, the electronic properties of the cobalt center of analogous C_1py and (DO)(DOH)pn (with added nitrogen ligands) alkyl derivatives are similar. Therefore, measurements of Co–C BDEs for these systems under identical conditions could give a clear assessment of the importance of the steric butterfly bending in Co–C bond homolysis.

Acknowledgment. We are grateful to the National Institutes of Health (GM 29225) for financial support. We also thank Drs. C. L. Hill for the use of the electrochemistry equipment, L. Randaccio for communicating unpublished results, and D. A. Sweigart for helpful discussions.

Supplementary Material Available: Details of the X-ray structural analysis, crystal packing diagrams, tables of positional parameters, bond lengths and angles, calculated H atom coordinates, and anisotropic thermal parameters, NMR data and analytical results, and CV data for **5–7** and **9–12** at scan rates 0.05–1 V/s, figures of the CV of **5** at 0.2 V/s, of **6** at 0.1, 0.2, and 0.5 V/s, of **11** at 1 and 0.2 V/s, of **12** at 0.2 V/s, of **9** at 0.2 V/s, and of **10** at 0.2 V/s (37 pages); listing of observed and calculated structure factors (32 pages). Ordering information is given on any current masthead page.

(33) For R = *neo*-C_5H_{11}, the $E_{1/2}$ values were used in the correlation since these values were available for both compounds. For X = CN, the E_{pc} values were used. Since only the E_{pc} value was available for [CH_3Co(C_1py)]ClO_4, we correlated this value, and the E_{pc} value for MeCbl (−1.94 V) calculated from $E_{1/2}$ and ΔE_p. The formal potential of chloroCbl, derived theoretically (−0.48 V),[22b] is the only Cbl redox potential that is more anodic than that of the corresponding C_1py derivative. However, a very good correlation could be obtained by using the experimental E_{pc} values of chloroCbl (−0.85 V, obtained from the reported CV[22b]) and of [ClCo(C_1py)]ClO_4 (−0.63 V). The E_{pa} value for [CH_3CNCo(C_1py)]$^{2+}$ (Table III) was obtained from the CVs of both [CH_3Co(C_1py)]ClO_4 and [CF_3CH_2Co(C_1py)]ClO_4. This peak is probably due to a reversible process, since its potential does not depend on the scan rate. Therefore, we could calculate the corresponding $E_{1/2}$ value (+0.08 V) and use this value along with the $E_{1/2}$ value for aquoCbl (−0.33 V)[22d] for solvato species in the correlation.